× 10^{-2} mmol), $Mn_2(CO)_{10}$ (2 mg, 5.13 × 10^{-3} mmol), and 0.2 mL of benzene-d_6 was prepared and sealed under vacuum. The initial NMR prior to photolysis showed that some reaction (about 63%) had occurred between $HMn(CO)_5$ and PPh_3 to give $HMn(CO)_4PPh_3$ (δ −6.9, d, J_{PH} = 35 Hz).[49] The tube, shielded from light during the initial reaction period, was then photolyzed for 2 min (see above for details). A decrease in both Ph_3PAuCH_3 methyl and $HMn(CO)_5$ hydride integrals relative to the phenyl region integration (which should remain constant) was observed; the **1**/$HMn(CO)_4PPh_3$ ratio thereby indicated was 1:9. A small peak at δ 0.18 due to methane was also now present. The product $HMn(CO)_4PPh_3$ was identified by its infrared spectrum in the carbonyl region (CCl_4, 1962 s, 2057 s).[49]

(49) Hieber, W.; Duchatsch, H. *Chem. Ber.* **1965**, *98*, 2933.

Acknowledgment. This research was supported by NSF Grants CHE82-07597 and CHE85-16415. The authors are grateful to Karen M. Hennessy for assistance with the CH_3AuPPh_3/$H_2Os(CO)_4$ photolysis.

Registry No. 1, 14692-78-5; **2**, 99747-68-9; **4**, 99782-58-8; $H_2Os_2(CO)_8$, 25685-05-6; $H_2Os(CO)_4$, 22372-70-9; Ph_3PAuCH_3, 23108-72-7; *cis*-$H_2Os(CO)_4$, 18972-42-4; $HRe(CO)_5$, 16457-30-0; $Re_2(CO)_{10}$, 14285-68-8; $HRe(CO)_4PPh_3$, 25838-69-1; $HMn(CO)_5$, 16972-33-1; $Mn_2(CO)_{10}$, 10170-69-1.

Experimental Characterization of an Electron-Rich ($\sigma^2\pi^4\delta^2\delta^{*2}$) Metal–Metal Triple Bond. Synthesis, Reactivity, and Photoelectron Spectral Studies of Trimethylphosphine Complexes of Dirhenium(II)

Dawn R. Root,[1a] Charles H. Blevins,[1b] Dennis L. Lichtenberger,*[1b] Alfred P. Sattelberger,[1c] and Richard A. Walton*[1a]

Contribution from the Department of Chemistry, Purdue University, West Lafayette, Indiana 49707, Laboratory for Electron Spectroscopy and Surface Analysis, Department of Chemistry, University of Arizona, Tucson, Arizona 85721, and the Los Alamos National Laboratory, Los Alamos, New Mexico 87545. *Received August 23, 1985*

Abstract: The reaction of $(n\text{-}Bu_4N)_2Re_2X_8$ (X = Cl or Br) with PMe_3 gives high yields of the triply bonded complexes $Re_2X_4(PMe_3)_4$. These compounds are oxidized by $NOPF_6$ to give paramagnetic $[Re_2X_4(PMe_3)_4]PF_6$, and the chloro derivative reacts with $Ph_2PCH_2PPh_2$ (dppm) and $Ph_2PNHPPh_2$ (dppa) to give $Re_2Cl_4(PMe_3)_2$(dppm) and $Re_2Cl_4(PMe_3)_2$(dppa), respectively. NMR spectroscopy (^1H and $^{31}P\{^1H\}$) shows that the latter complexes possess fairly symmetrical structures in which the PMe_3 ligands are in cis dispositions with respect to the bridging dppm and dppa ligands. The volatility of $Re_2Cl_4(PMe_3)_4$ has permitted the measurement of its gas-phase photoelectron spectrum which accords with this compound possessing a $\sigma^2\pi^4\delta^2\delta^{*2}$ configuration. The δ^* ionization band is slightly narrower than the δ ionization band and occurs at about 0.9 eV lower binding energy. The π ionization gives evidence of spin–orbit splitting as expected for the heavy-atom rhenium character. An ionization assigned to removal of an electron from the valence σ orbital is observed at a binding energy 1 eV higher than the π ionization. Comparison of these ionizations with those of the corresponding $W_2Cl_4(PMe_3)_4$ ($\sigma^2\pi^4\delta^2$) complex is especially informative. In particular, these observations support a strong interaction between the valence σ density on one metal atom and the core density on the neighboring metal atom in these complexes.

Complexes with close metal–metal interactions offer special opportunities to investigate the factors that influence metal–metal bonding, electronic structure, and reactivity.[2] Quadruply bonded complexes, which are derived from d^4–d^4 metal interactions and have the $\sigma^2\pi^4\delta^2$ configuration, are especially interesting because they provide occupied orbitals with each symmetry type of metal–metal interaction—σ, π, and δ. Also interesting are species which are related by either the addition or removal of electrons from the $\sigma^2\pi^4\delta^2$ configuration. In particular, "electron-poor" metal–metal triple bonds derived from d^3–d^3 complexes with $\sigma^2\pi^4$ configurations, and "electron-rich" metal–metal triple bonds derived from d^5–d^5 complexes with $\sigma^2\pi^4\delta^2\delta^{*2}$ configurations,[2] serve to expand our knowledge of the range of metal–metal interactions.

Valence photoelectron spectroscopy (PES) has proven to be extremely valuable in providing insight into the electronic interactions in metal–metal bonds, particularly for the quadruple[3–7] and electron-poor triple[8,9] metal–metal bonds. Nonetheless, important questions remain concerning the nature of the δ-ionized

(1) (a) Purdue University. (b) University of Arizona. (c) Los Alamos National Laboratory.

(2) Cotton, F. A.; Walton, R. A. "Multiple Bonds Between Metal Atoms"; Wiley: New York, 1982.

(3) (a) Reference 2, pp 415–425, and references therein. (b) Cowley, A. H. *Prog. Inorg. Chem.* **1979**, *26*, 46.

(4) (a) Cotton, F. A.; Norman, J. G., Jr.; Stults, B. R.; Webb, T. R. *J. Coord. Chem.* **1976**, *5*, 217. (b) Coleman, A. W.; Green, J. C.; Hayes, A. J.; Seddon, E. A.; Lloyd, D. R.; Niwa, Y. *J. Chem. Soc., Dalton Trans.* **1979**, 1057. (c) Garner, C. D.; Hillier, I. H.; Knight, M. J.; McDowell, A. A.; Walton, I. B.; Guest, M. F. *J. Chem. Soc., Faraday Trans. 2* **1980**, *76*, 885. (d) Garner, C. D.; Hillier, I. H.; MacDowell, A. A.; Walton, I. B.; Guest, M. F. *Ibid.* **1979**, *75*, 485. (e) Berry, M.; Garner, C. D.; Hillier, I. H.; MacDowell, A. A.; Walton, I. B. *Chem. Phys. Lett.* **1980**, *70*, 350. (f) Bursten, B. E.; Cotton, F. A.; Cowley, A. H.; Hanson, B. E.; Lattman, M.; Stanley, G. G. *J. Am. Chem. Soc.* **1979**, *101*, 6244.

(5) (a) Bancroft, G. M.; Pellach, E.; Sattelberger, A. P.; McLaughlin, K. W. *J. Chem. Soc., Chem. Commun.* **1982**, 752. (b) Sattelberger, A. P. In "Inorganic Chemistry: Towards the 21st Century"; Chisholm, M. H., Ed.; American Chemical Society: Washington, DC, **1983**, p 291.

(6) (a) Lichtenberger, D. L., ref 5b, p 221. (b) Lichtenberger, D. L.; Blevins, C. H., II *J. Am. Chem. Soc.* **1984**, *106*, 1636. (c) Blevins, C. H., II *Diss. Abstr. Intl.* **1984**, *45*, 1186 B (see Chapters 5 and 6).

(7) Cotton, F.A.; Hubbard, J. L.; Lichtenberger, D. L.; Shim, I. *J. Am. Chem. Soc.* **1982**, *104*, 679.

(8) (a) Cotton, F. A.; Stanley, G. G.; Kalbacher, B. J.; Green, J. C.; Seddon, E.; Chisholm, M. H. *Proc. Natl. Acad. Sci. U.S.A.* **1977**, *74*, 3109. (b) Bursten, B. E.; Cotton, F. A.; Green, J. C.; Seddon, E. A.; Stanley, G. G. *J. Am. Chem. Soc.* **1980**, *102*, 4579.

0002-7863/86/1508-0953$01.50/0

Table I. Electrochemical and NMR Spectral Data for $Re_2Cl_4(PMe_3)_2(LL)$ Complexes (LL = dppm or dppa)

complex	$E_{p,a}$[a]	$E_{1/2}(ox)$[a]	NMR spectra	
			^1H,[d] δ	^{31}P,[e] δ
$Re_2Cl_4(PMe_3)_2(dppm)$	+1.28	+0.58	1.45 (d, CH_3, ^2J(P-H) = 10.2 Hz), 6.35 (t, $-CH_2-$, ^2J(P-H) = 10.4 Hz)	+1.71 (s) -24.76 (m)
$Re_2Cl_4(PMe_3)_2(dppa)$	+1.26	+0.65	1.48 (d, CH_3, ^2J(P-H) = 10.4 Hz)	+53.42 (s) -25.80 (m)
$Re_2Cl_4(PMe_2Ph)_2(dppa)$	+1.37[b]	+0.64[b]		
$Re_2Cl_4(PEt_3)_2(dppm)$	+1.15	+0.55[c]		

[a] Volts vs. Ag/AgCl using a Pt-bead electrode in CH_2Cl_2–0.2 M TBAH at ν = 200 mV/s. [b] Volts vs. SCE in CH_2Cl_2–0.2 M TBAH (see ref 28). [c] Irreversible; $E_{p,a}$ value given. [d] Recorded in CD_2Cl_2; d = doublet, t = triplet. [e] Recorded in CD_2Cl_2/CH_2Cl_2; s = singlet, m = multiplet.

state, the implications of spin–orbit splitting in the π ionization, and the identification of the σ-bond ionization. Photoelectron studies of electron-rich triple bonds, with the $\sigma^2\pi^4\delta^2\delta^{*2}$ configuration, are likely to yield key additional information for interpreting the spectra of each class of these complexes and understanding their metal–metal bonding.[2,10] In particular, occupation of the δ^* orbital offers the opportunity to directly observe the effects of removing an electron from this antibonding orbital. Also, these electron-rich complexes do not possess the same low-lying excited states that can produce the configuration interaction complexities of quadruply bonded systems. This can have important influences on features in the photoelectron spectrum.[11]

Complexes of the type $Re_2X_4(PR_3)_4$ (X = Cl, Br, or I; PR_3 = monodentate phosphine) constitute the best known examples of the electron-rich metal–metal triple bond.[2,12,13] Among the most recent studies on these compounds have been ones that dealt with their spectroscopic properties and electronic structure,[10] their redox chemistry,[14] and their reactions with π-acceptor ligands.[15] However, none of the complexes studied to date have displayed any significant degree of volatility thereby precluding a study of their gas-phase chemistry. While we had prepared the trimethylphosphine complex $Re_2Cl_4(PMe_3)_4$ some years ago,[12] its properties and chemical reactivity have not been examined previously since we had anticipated that they would not differ to any significant extent from those of other complexes of this type. Consequently, interest in this molecule has remained dormant. However, very recent studies have revealed that this complex possesses sufficient volatility to permit the measurement of its gas-phase photoelectron spectrum (PE), thereby providing the first such data for a complex of this type. This complex is particularly significant because it can be compared directly with the quadruply bonded complex $W_2Cl_4(PMe_3)_4$ ($\sigma^2\pi^4\delta^2$), which has been studied previously by photoelectron spectroscopy and SCF-Xα calculations.[7] It turns out that the PE spectrum of $Re_2Cl_4(PMe_3)_4$ provides some key information for interpreting the interactions between multiply bonded transition metal atoms in general. These results, along with a more complete characterization of $Re_2Cl_4(PMe_3)_4$ and its previously unreported bromide analogue, are described in the present report.

Experimental Section

Starting Materials. The complexes $(n\text{-}Bu_4N)_2Re_2X_8$, where X = Cl or Br, were prepared according to standard literature procedures.[16,17] All solvents and reagents were obtained from commercial sources and used without further purification. Solvents were dried with use of standard techniques and deoxygenated by a nitrogen purge.

Reaction Procedures. All reactions were carried out under a dry nitrogen atmosphere with use of vacuum line techniques.

A. Preparation of $Re_2X_4(PMe_3)_4$. (i) X = Cl. This compound was prepared via a previously reported method[12] with one important variation. The reaction mixture was refluxed for 3 days instead of the reported 10 days. Emerald green crystals were obtained; yield 75–80%. Anal. Calcd for $C_{12}H_{36}Cl_4P_4Re_2$: C, 17.61; H, 4.44. Found: C, 17.77; H, 4.24.

(ii) X = Br. Trimethylphosphine (1.0 mL) was added to a mixture of $(n\text{-}Bu_4N)_2Re_2Br_8$ (0.499 g, 0.333 mmol) in *n*-propyl alcohol (10 mL). The green-brown reaction mixture was refluxed for 2 days. The resulting emerald green crystals were filtered off, washed with *n*-propyl alcohol and diethyl ether, and dried in vacuo; yield 0.256 g (77%). Anal. Calcd for $C_{12}H_{36}Br_4P_4Re_2$: C, 14.46; H, 3.65. Found: C, 14.74; H, 3.58.

B. Oxidation of $Re_2X_4(PMe_3)_4$. (i) X = Cl. $Re_2Cl_4(PMe_3)_4$ (0.117 g, 0.143 mmol) was suspended in 2.0 mL of acetonitrile at 0 °C. $NOPF_6$ (0.033 g, 0.189 mmol) was added and the mixture was stirred at 0 °C for 10 min. The ice bath was removed and stirring was continued for 10 min at room temperature. Diethyl ether (10 mL) was added to initiate precipitation of the product. The violet-brown powder was filtered off, washed with diethyl ether, and dried in vacuo; yield 0.111 g (80%). Anal. Calcd for $C_{12}H_{36}Cl_4F_6P_5Re_2$: C, 14.96; H, 3.77. Found: C, 14.96; H, 3.97.

(ii) X = Br. $Re_2Br_4(PMe_3)_4$ (0.103 g, 0.103 mmol) was suspended in acetonitrile (3.0 mL) at 0 °C. $NOPF_6$ (0.025 g, 0.143 mmol) was added and the reaction mixture was stirred at 0 °C for 5 min. The ice bath was removed and stirring was continued for several minutes. Diethyl ether (10 mL) was added and the mixture was stirred at room temperature for 2 h. Hexane was added until precipitation began. The brown powder was filtered off, washed with hexane, and dried in vacuo; yield 0.075 g (64%). Anal. Calcd for $C_{12}H_{36}Br_4F_6P_5Re_2$: C, 12.63; H, 3.19. Found: C, 13.20; H, 3.26.

C. Reactions of $Re_2Cl_4(PMe_3)_4$. (i) Reaction with Bis(diphenylphosphino)methane (dppm). A mixture of $Re_2Cl_4(PMe_3)_4$ (0.050 g, 0.061 mmol) and dppm (0.047 g, 0.122 mmol) was suspended in 10 mL of toluene and refluxed for 4 days. The resulting violet crystals were washed with diethyl ether and dried in vacuo; yield 0.047 g (73%). This reaction was also carried out with benzene as solvent but with a much lower yield. Anal. Calcd for $C_{31}H_{40}Cl_4P_4Re_2$: C, 35.43; H, 3.84. Found: C, 36.27; H, 3.85.

(ii) Reaction with Bis(diphenylphosphino)amine (dppa). A mixture of $Re_2Cl_4(PMe_3)_4$ (0.056 g, 0.068 mmol) and dppa (0.070 g, 0.182 mmol) was suspended in 10 mL of toluene and refluxed for 18 h. The resulting gray-violet powder was washed with diethyl ether and dried in vacuo; yield 0.058 g (81%). Anal. Calcd for $C_{30}H_{39}NCl_4P_4Re_2$: C, 34.26; H, 3.75; Cl, 13.42. Found: C, 33.89; H, 3.66; Cl, 13.62.

Photoelectron Spectral Measurements. The photoelectron spectra were obtained with use of a spectrometer featuring a 36-cm-radius hemispherical analyzer and other improvements described previously.[18,19] The spectra were measured at 190 °C with use of the argon ionization at 15.759 eV as an internal calibration lock. The energy scale drift during data collection was maintained at less than ±0.03 eV. Spectra of the full valence region as well as individual close-up regions were repeated after periods of several months, and no changes in spectral details could be detected. The ionization bands are well-represented in simple analytical form in Table II with asymmetric Gaussian band shapes determined by their position, relative amplitude, and bandwidths at half-heights as indicated by the high binding energy (W_H) and low binding energy (W_L) sides of each peak.

(9) Kober, E. M.; Lichtenberger, D. L. *J. Am. Chem. Soc.* **1985**, *107*, 7199.
(10) Bursten, B. E.; Cotton, F. A.; Fanwick, P. E.; Stanley, G. G.; Walton, R. A. *J. Am. Chem. Soc.* **1983**, *105*, 2606.
(11) Lichtenberger, D. L. "Abstracts", 187th ACS Meeting, St. Louis, 1984, INOR 48.
(12) Ebner, J. R.; Walton, R. A. *Inorg. Chem.* **1975**, *14*, 1987.
(13) Cotton, F. A.; Frenz, B. A.; Ebner, J. R.; Walton, R. A. *Inorg. Chem.* **1976**, *15*, 1630.
(14) Cotton, F. A.; Dunbar, K. R.; Falvello, L. R.; Tomas, M.; Walton, R. A. *J. Am. Chem. Soc.* **1983**, *105*, 4950.
(15) See, for example: Dunbar, K. R.; Walton, R. A. *Inorg. Chim. Acta* **1984**, *87*, 185.
(16) Barder, T. J.; Walton, R. A. *Inorg. Chem.* **1982**, *21*, 2510.
(17) Cotton, F. A.; Curtis, N. F.; Johnson, B. F. G.; Robinson, W. R. *Inorg. Chem.* **1965**, *48*, 326.
(18) Calabro, D. C.; Hubbard, J. L.; Blevins, C. H., II; Campbell, A. C.; Lichtenberger, D. L. *J. Am. Chem. Soc.* **1981**, *103*, 6839.
(19) Lichtenberger, D. L.; Calabro, D. C.; Kellogg, G. E. *Organometallics* **1984**, *3*, 1623.

Table II. Valence Ionization Band Positions and Half-Widths for $Re_2Cl_4(PMe_3)_4$

position eV	W_H[a]	W_L[a]	relative area	assignment[b]	state
5.66	0.38	0.31	1.0	$3a_2$, M-Mδ*	$^2A_2$
6.51	0.41	0.34	1.0	$3b_1$, M-Mδ	$^2B_1$
7.78[c]	0.53	0.38	1.1	9e, M-Mπ	$^2E_{3/2}$
8.09[c]	0.53	0.38	1.1		$^2E_{1/2}$
8.49	0.36	0.33	1.9	8e, Pσ	$^2E_{3/2,1/2}$
8.83[c]	0.48	0.39	1.3	$7a_1$, M-Mσ[d]	$^2A_1$
10.01	0.84	0.39	~10	Cl lone pairs	(several)
~11				$6a_1$, M-Cl, M-Pσ	$^2A_1$

[a] Assymmetric Gaussian peak widths as indicated on the high binding energy (W_H) and low binding energy (W_L) sides. The full peak width at half-height is $(W_H + W_L)/2$. [b] See text for a more complete explanation of ionization character. [c] Standard deviations in the positions and widths of single, isolated ionizations are about 0.01 eV and the relative areas are reproducible to about 5%. In these cases of overlapping ionizations there is greater uncertainty in individual positions, widths, and intensities although the overall band contour is accurately represented as shown in Figure 3. [d] This corresponds to the $3a_1$ of ref 10.

Other Physical Measurements. Infrared spectra were recorded as Nujol mulls with an IBM IR/32 Fourier transform spectrometer (4000–400 cm^{-1}) and a Digilab FTS-20B spectrometer (500–50 cm^{-1}). Electronic absorption spectra were recorded as CH_2Cl_2 solutions on Cary 17D and IBM 9420 spectrophotometers. Electrochemical experiments were performed by using a Bioanalytical Systems, Inc., Model CV-1A instrument in conjunction with a Hewlett-Packard Model 7035B *x–y* recorder. Dichloromethane solutions containing 0.2 M tetra-*n*-butylammonium hexafluorophosphate (TBAH) as a supporting electrolyte were utilized. $E_{1/2}$ values $[(E_{p,a} + E_{p,c})/2]$ were referenced against a Ag/AgCl electrode at room temperature and were uncorrected for junction potentials. ^{31}P NMR and ^1H NMR spectra were recorded on CD_2Cl_2 solutions with a Varian XL-200 spectrometer. X-Band ESR spectra of dichloromethane solutions were recorded at −160 °C with a Varian E-109 spectrometer. Conductivity measurements were performed on 1×10^{-3} M acetonitrile solutions with an Industrial Instruments, Inc., Model RC-16B2 conductivity bridge. Magnetic susceptibility measurements were done by the Evans method[20,21] in dichloromethane on a 90-MHz Perkin-Elmer spectrometer. Diamagnetic corrections were estimated from Pascal's constants. Mass spectral and FAB data were obtained through the Purdue University mass spectral service facility. The EI mass spectra, which were measured at 70 eV on a Finnigan 4000 mass spectrometer, were obtained by a direct probe insertion method (probe temperature of 150 °C) with a source temperature of 250 °C. The CI mass spectra were measured on this same instrument with butane gas. The fast atom bombardment (FAB) spectra were recorded on glycerol solutions with a Kratos MS-50 spectrometer.

Analytical Procedures. Elemental microanalyses were performed by Dr. H. D. Lee of the Purdue University microanalytical laboratory.

Results and Discussion

(a) Synthesis and Characterization of $Re_2X_4(PMe_3)_4$ (X = Cl or Br). These two emerald green complexes can be prepared in good yield (ca. 80%) by the direct reaction of PMe_3 with $(n\text{-}Bu_4N)_2Re_2X_8$, a procedure which has been used previously[12] to prepare other complexes of this type. The Nujol mull IR (400–150 cm^{-1}) and solution electronic absorption spectra of these two complexes resemble very closely the corresponding spectral properties reported for other complexes of this type,[12,14] thereby confirming their structural identity (see I).[22] This is further

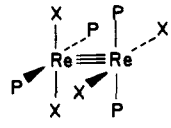

I

(X = Cl or Br; P = PR_3)

confirmed by the electrochemical properties of these two complexes. As expected for complexes that possess the $\sigma^2\pi^4\delta^2\delta^{*2}$ configuration, solutions of $Re_2X_4(PMe_3)_4$ in 0.2 M TBAH–CH_2Cl_2 exhibit two one-electron oxidations in their cyclic voltammograms. The $E_{1/2}$ values for these reversible processes ($E_{1/2}$ = −0.23 and +0.96 V vs. Ag/AgCl for X = Cl, and $E_{1/2}$ = −0.11 and +1.01 V vs. Ag/AgCl for X = Br) are typical of $Re_2X_4(PR_3)_4$-type compounds.[14,23]

The $^{31}P\{^1H\}$ NMR spectra of these complexes (recorded in CD_2Cl_2) have singlets at δ −21.51 and −30.15 for the chloro and the bromo derivatives, respectively.[24] This result is of course expected for the symmetric structure I but is noteworthy for being the first such study of the ^{31}P NMR of a complex of the type $Re_2X_4(PR_3)_4$. The ^1H NMR spectra also support a symmetric structure; while the chloro derivative gives a singlet at δ 1.29 in its spectrum, the bromo derivative possesses a triplet at δ 1.51 with use of resolution enhancement. This splitting is apparently due to a P–H coupling (3.7 Hz) that is not apparent in the case of the chloride analogue.

The CI mass spectrum of $Re_2Cl_4(PMe_3)_4$ showed a base peak at *m/e* 77, corresponding to $(Me_3PH)^+$, together with the parent ion (M^+) at *m/e* 818 (25% abundance) and $(M - PMe_3)^+$ at *m/e* 742 (5% abundance). The corresponding EI mass spectrum was similar but lacked the parent ion multiplet and now had *m/e* 742 as the base peak. A quite intense peak at *m/e* 666 (65% abundance) corresponded to the ion $(M - 2PMe_3)^+$. The corresponding CI and EI mass spectra of $Re_2Br_4(PMe_3)_4$ show a peak at *m/e* 843 due to the ion $[Re_2Br_4(PMe_3)_2]^+$ (i.e., $(M - 2PMe_3)^+$) and a peak at *m/e* ~996 (the limit of our accessible mass range) that characterized the parent ion. Clearly then, these properties demonstrate that the structural integrity of the dirhenium unit is maintained in the gas phase and indicated to us the feasibility of studying the photoelectron spectra of these complexes (see section d).

(b) Oxidation of $Re_2X_4(PMe_3)_4$. On the basis of the electrochemistry of these complexes, as discussed in the preceding section, chemical oxidation to the monocations could be anticipated. This was accomplished by using $NOPF_6$ dissolved in acetonitrile. The resulting brown solids had microanalytical data in accord with the formulation $[Re_2X_4(PMe_3)_4]PF_6$. The cyclic voltammograms of 0.2 M TBAH–CH_2Cl_2 solutions of these complexes confirmed that a one-electron oxidation had indeed occurred (the couple at $E_{1/2} \simeq -0.15$ V corresponded to a one-electron reduction, while that at $E_{1/2} \simeq +1.0$ V vs. Ag/AgCl is still an oxidation).

The magnetic moments of CH_2Cl_2 solutions of the complexes were found to be 1.60 and 1.75 μ_B for the chloro and bromo derivatives, respectively. These values are consistent with one unpaired electron, which would of course be the case for the monocations if they possess the $\sigma^2\pi^4\delta^2\delta^{*1}$ ground-state electronic configuration. Their paramagnetic nature is also reflected by the X-band ESR spectra of these complexes (measured in CH_2Cl_2 at −160 °C) which reveal a fairly isotropic, albeit broad, signal (peak to peak separation of ~400 G) at g_{av} = 2.41–2.42. This contrasts with the complex, anisotropic pattern showing hyperfine

(20) Evans, D. F. *J. Chem. Soc.* **1959**, 2003.
(21) Deutsch, J. L.; Poling, S. M. *J. Chem. Educ.* **1969**, *46*, 167.
(22) Spectroscopic properties are as follows: X = Cl, IR spectrum (Nujol mull) ν(Re–Cl) 320 (s) and 298 (s) cm^{-1}, other bands at 340 (s), 225 (m), and 195 (s) cm^{-1}; electronic absorption spectrum (CH_2Cl_2, ϵ_{max} in parentheses) 732 (sh), 635 (sh), 613 (210), 519 (100), 466 (105), and 401 (180) nm. X = Br, IR spectrum (Nujol mull) 340 (s), 277 (w), 204 (w?), 199 (w?), and 184 (s) cm^{-1}; electronic absorption spectrum (CH_2Cl_2, ϵ_{max} in parentheses) 785 (sh), 654 (210), 625 (205), 485 (90), and 415 (150) nm.
(23) Brant, P.; Salmon, D. J.; Walton, R. A. *J. Am. Chem. Soc.* **1978**, *100*, 4424.
(24) $^{31}P\{^1H\}$ NMR spectra were recorded with aqueous 85% H_3PO_4 as an external standard. Positive chemical shifts are downfield from H_3PO_4.

structure that is observed for other $[Re_2X_4(PR_3)_4]^+$ species.[14,23] This difference may reflect a difference in relaxation rates or in the rate of tumbling of these molecules in the dichloromethane glass. The $\delta \rightarrow \delta^*$ transition, which characterizes dimetal species that possess the $\sigma^2\pi^4\delta^2\delta^{*1}$ configuration,[10,14,25] is seen at 1380 nm (X = Cl) and 1418 nm (X = Br), with ϵ = 4000–4500, in the electronic absorption spectra of CH_2Cl_2 solutions of $[Re_2X_4(PMe_3)_4]PF_6$.[26] Solutions of these complexes in acetonitrile have conductivities (Λ_m = 125–140 ohm^{-1} cm^2 mol^{-1} for $c_m = 1 \times 10^{-3}$ M) which accord with their being 1:1 electrolytes.

The FAB mass spectrum of $[Re_2Cl_4(PMe_3)_4]PF_6$ (in glycerol) is particularly well defined. It shows the parent cation at *m/e* 818 (the base peak) together with quite intense fragment peaks at *m/e* 783, 742, 707, 666, and 630 produced by the loss of chloride and phosphine ligands. This gas-phase stability accords with the mass spectral results for $Re_2X_4(PMe_3)_4$ (see section a).

(c) Reactions of $Re_2Cl_4(PMe_3)_4$ with $Ph_2PCH_2PPh_2$ and $Ph_2PNHPPh_2$. Upon exploring the substitutional lability of the PMe_3 ligands of $Re_2Cl_4(PMe_3)_4$, we examined the reactions of this complex with dppm and dppa. Reaction in boiling toluene gave the violet colored solids $Re_2Cl_4(PMe_3)_2$(dppm) and $Re_2Cl_4(PMe_3)_2$(dppa). These complexes are apparently examples of a type of mixed phosphine complex made previously on only two occasions, namely, $Re_2Cl_4(PEt_3)_2$(dppm)[27] and $Re_2Cl_4(PMe_2Ph)_2$(dppa).[28] The similarity between the low-frequency IR and electronic absorption spectral properties of these two complexes[27,28] implies a close similarity in structure. In turn, we find that CH_2Cl_2 solutions of $Re_2Cl_4(PMe_2Ph)_2$(dppa)[28] and $Re_2Cl_4(PMe_3)_2$(dppa) have essentially the same electronic absorption spectra[29] and that the low-frequency IR spectrum of $Re_2Cl_4(PMe_3)_2$(dppm) (ν(Re–Cl) at ~305 and 280 cm^{-1}) closely resembles the spectra reported previously for $Re_2Cl_4(PEt_3)_2$(dppm)[27] and $Re_2Cl_4(PMe_2Ph)_2$(dppa).[28] Finally, this structural similarity is further supported by the electrochemical properties of all four complexes under consideration (see Table I). Each complex possesses two one-electron oxidations, the first of which is quasireversible, while that at higher positive potentials is irreversible. The occurrence of two oxidation processes is typical of complexes that are derivatives of the triply bonded Re_2^{4+} core.[23,28]

The NMR spectral properties of these complexes provide convincing evidence that these complexes possess the structure depicted in II. The ^{1}H NMR spectra (recorded in CD_2Cl_2) show a doublet for the methyl resonances of the PMe_3 ligands (Table I) with ^2J(P–H) ≃ 10.3 Hz and, in the case of the dppm complex, a triplet at δ 6.35 (^2J(P–H) ≃ 10.4 Hz) arising from the single bridgehead methylene. The phenyl resonances are located between δ 7.0 and 7.8; on the basis of decoupling experiments the ortho protons of the inequivalent sets of phenyl rings are seen as multiplets at ca. δ 7.1 and 7.6, while the meta and para protons are centered around δ 7.4. In the case of the dppa complex, the latter feature is split into two clear sets of multiplets that are due to the meta and para protons of the inequivalent phenyl rings.

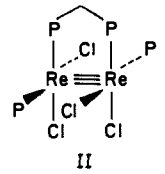

II

(P = PR_3; P P = dppm or dppa)

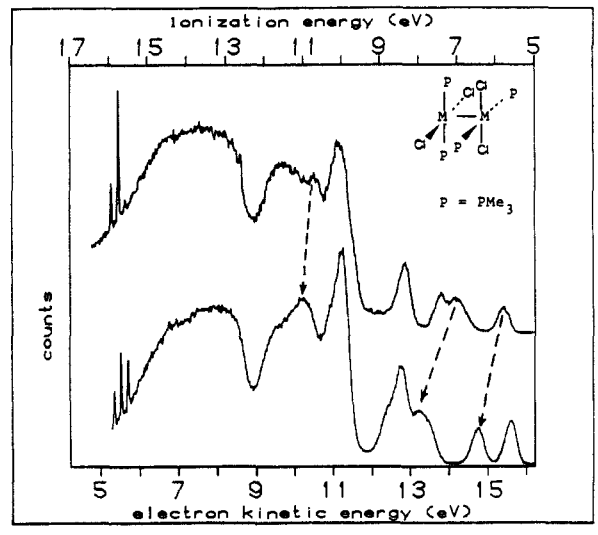

Figure 1. The full He I valence photoelectron spectra of $W_2Cl_4(PMe_3)_4$ (top) and $Re_2Cl_4(PMe_3)_4$ (bottom). The sharp features near 16 eV ionization energy are from argon and nitrogen internal standards. The dashed lines indicate the shifts of particular ionization features.

The ^{31}P NMR spectra of both complexes are quite simple (Table I). A downfield singlet is attributed to the phosphorus atoms of the dppm and dppa ligands, while a multiplet at δ –25 (actually a 1:9:36:84:126:126:84:36:9:1 pattern) is due to the phosphorus of the PMe_3 ligands (^2J(P–H) = 10.4 Hz). The corresponding ^{31}P{^{1}H} spectra show two singlets. Since there is no measurable P–P coupling, the phosphine donor atoms must be in a cis disposition to one another. This observation, coupled with a triplet for the proton resonance of the bridgehead –CH_2– of the dppm ligand (Table I), strongly favors II as being the correct structure.[30]

(d) Photoelectron Spectrum of $Re_2Cl_4(PMe_3)_4$. With this characterization of the physical and chemical properties of the $Re_2X_4(PMe_3)_4$ complexes it is now possible to evaluate in detail a characteristic photoelectron spectrum of an electron-rich metal–metal triple bond. The $Re_2Cl_4(PMe_3)_4$ complex sublimes cleanly at about 190 °C with enough vapor pressure in our spectrometer to obtain an extremely high quality valence photoelectron spectrum. The sensitivity is sufficiently high to make possible long, detailed examinations of individual regions of the spectrum. It is especially interesting to compare the valence photoelectron spectrum of $Re_2Cl_4(PMe_3)_4$, which has a formal metal–metal triple bond configuration of $\sigma^2\pi^4\delta^2\delta^{*2}$, with the previously published[7] photoelectron spectrum of the nearly isostructural ditungsten analogue, $W_2Cl_4(PMe_3)_4$, which has a formal metal–metal quadruple bond configuration of $\sigma^2\pi^4\delta^2$. The full valence spectra of these complexes from 5 to 17 eV are shown in Figure 1. Table II summarizes the individual band positions and relative areas of the ionizations of the rhenium complex from 5 to 11 eV. This table also includes assignments based on comparisons of these photoelectron spectra and on correlations with the previous SCF–Xα calculations on the rhenium[10] and tungsten[7] complexes.

The first notable feature in the spectrum of the rhenium complex is the appearance of the additional ionization band at the onset of the photoelectron spectrum between 5 and 6 eV ionization energy. This band is assigned to the $^2A_2$ positive ion state and correlates with ionization from the predominantly Re–Re δ^* symmetry orbital. Ionization from the δ bonding orbital ($^2B_1$ state) is observed at 0.85 eV greater binding energy than the δ^* ionization. This is in good agreement with the 0.9-eV separation of these positive ion states observed for the $\delta \rightarrow \delta^*$ transition in the solution electronic absorption spectrum of $[Re_2Cl_4(PMe_3)_4]^+$. It

(25) Ebner, J. R.; Walton, R. A. *Inorg. Chim. Acta* **1975**, *14*, L45.
(26) The low-frequency IR spectra (Nujol mull) of these complexes are as follows: X = Cl, ν(Re–Cl) 350 (s) and 310 (m s) cm^{-1}, other band at 382 (s) cm^{-1}; X = Br, 380 (s) cm^{-1}.
(27) Ebner, J. R.; Tyler, D. R.; Walton, R. A. *Inorg. Chem.* **1976**, *15*, 833.
(28) Barder, T. J.; Cotton, F. A.; Lewis, D.; Schwotzer, W.; Tetrick, S. M.; Walton, R. A. *J. Am. Chem. Soc.* **1984**, *106*, 2882.
(29) Absorption maxima (λ_{max}) are observed at 560 and 425 nm for $Re_2Cl_4(PMe_2Ph)_2$(dppa),[28] while for $Re_2Cl_4(PMe_3)_2$(dppa) we find bands at 581 (ϵ ~ 210) and 423 (ϵ ~ 325) nm.
(30) A less symmetrical structure, still maintaining a cis disposition of phosphines, with the two PMe_3 ligands on the same side of the molecule, would most likely give rise to an AB or AX pattern for the –CH_2– resonance. This is not observed.

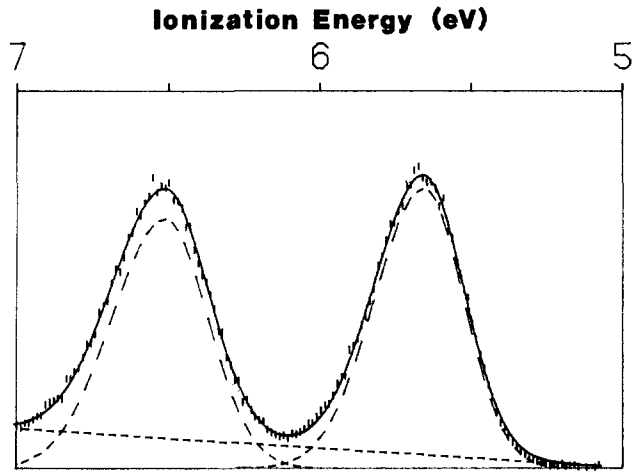

Figure 2. Close-up analysis of the first (δ^*) and second (δ) ionization bands of $Re_2Cl_4(PMe_3)_4$. The spectrum has been corrected for the instrument transmission function. The dashed lines are the individual asymmetric Gaussian peaks and the base line, and the solid line is the fit of the experimental data, which is represented by the vertical line segments.

is also in good agreement with the SCF-Xα calculations on $Re_2Cl_4(PH_3)_4$, which determined a 0.78-eV separation in the δ and δ^* orbital energies and a 0.70-eV energy for the $\delta \rightarrow \delta^*$ transition in the cation.[10]

A closer look at the δ^* and δ ionizations is provided in Figure 2. The δ^* ionization is only slightly more intense and narrow than the δ ionization, and the relative area of the two ionizations is the same within a few percent. From the energy separation and bandwidths it does not appear that ionization from the δ and δ^* orbitals is producing completely localized hole states, as might be expected if the δ symmetry interaction between the two metals was extremely weak.[31] Initial attempts at resolving vibrational fine structure in these bands (as in the case of $Mo_2(O_2CCH_3)_4$)[6] have not been successful. However, the slightly narrower δ^* ionization band does indicate that the equilibrium bond distance changes (associated with the vibrational progressions comprising the band envelopes) are slightly less for removal of an electron from the δ^* orbital than from the δ orbital.

Of course, factors other than the change in metal–metal bond order have strong influences on the bandwidths. It has been shown previously that the change in formal metal oxidation state is important in determining the total metal–metal interaction, and this change will be relatively similar for these two ionization processes.[6,10,32,33] Also, certain predominantly ligand vibrational progressions are likely to be activated by the ionization,[6,34] and this contribution to band broadening will also be relatively similar for both δ^* and δ ionization. Nonetheless, although the major contributions to the bandwidths may come from other sources, the observation that the δ^* ionization band is slightly narrower than the δ ionization band is consistent with removal of an antibonding electron in comparison to removal of a bonding electron.

There is considerable overlap of individual ionization features in the remaining portions of the photoelectron spectrum of $Re_2Cl_4(PMe_3)_4$. Careful comparison of this spectrum with that of the analogous tungsten complex allows identification of those ionizations associated with a substantial amount of metal character. It is important to remember that the larger effective nuclear charge for valence electrons of rhenium compared to tungsten will cause a relative increase in the ionization energies of comparable metal orbitals. As an example, this shift is clearly observed for the δ ionization, which occurs at 0.78 eV higher ionization energy in the rhenium complex than in the tungsten complex.

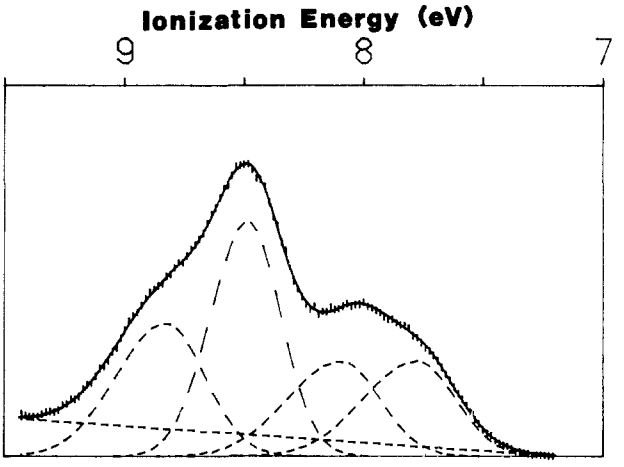

Figure 3. Close-up analysis of the 7–9 eV ionization energy region of $Re_2Cl_4(PMe_3)_4$. The spectrum has been corrected for the instrument transmission function. The dashed lines are the individual asymmetric Gaussian peaks and the base line, and the solid line is the fit of the experimental data, which is represented by the vertical line segments.

A close-up spectrum of the 7–9 eV ionization energy region of the rhenium complex is shown in Figure 3. At least four ionization bands are overlapping in this region. The most intense component in this region, located at 8.49 eV, correlates with ionization from the 8e orbital.[7,10] This ionization is largely associated with the phosphorus lone pairs, and there is apparently little metal character involved. The energy of this ionization is the same (8.42 ± 0.07 eV) in the spectra of the molybdenum, tungsten, and rhenium analogues, and there is no evidence of spin–orbit splitting or broadening as would be caused by a third row metal character in this ionization. Previous He I/He II intensity comparisons on the molybdenum and tungsten complexes also indicated little metal character associated with this ionization.[7]

The leading edge of this region, between 7.2 and 8.2 eV, shows a broad ionization feature with a flat slope on the top. This feature is assigned to the predominantly metal–metal π ionization (9e orbital). It occurs as expected at about 0.7–1.0 eV greater ionization energy than the corresponding ionization of the tungsten complex. The center of this band is at 1.42 eV greater binding energy than that of the δ ionization. This is in excellent agreement with the SCF-Xα calculations, which obtain a 1.41-eV separation in these orbital energies. Analysis of the band shape shows that it is accurately represented by two equal components separated by 0.3 eV, indicating the expected spin–orbit splitting of the π ionization into the $E_{1/2}$ and $E_{3/2}$ states. This splitting is near that expected for atomic rhenium,[35] indicating the relatively pure metal character associated with the 9e ionization, as was also observed in the He I/He II spectral comparisons of the molybdenum and tungsten analogues.[7]

The SCF-Xα calculations indicate a large amount of metal–ligand mixing in the ground-state orbitals of e symmetry.[10] Furthermore, the SCF-Xα calculation on the positive ion shows that the mixing is not significantly changed with the increase in the effective oxidation state of rhenium, indicating that electron relaxation effects are not responsible for creating the relatively pure phosphorus or metal character in the 8e and 9e ion states. It has been noted that the 8e and 9e orbitals together produce a phosphorus lone pair e orbital that is basically nonbonding with the metal. This combination of the phosphorus lone pair orbitals interacts primarily with atomic p orbitals on the metal centers. The mixing indicated by the calculations of this phosphorus lone

(31) (a) Cotton, F. A. *Pure Appl. Chem.* **1980**, *52*, 2331. (b) Benard, M. *J. Am. Chem. Soc.* **1978**, *100*, 2354. (c) Upton, T. H.; Goddard, W. A., III *J. Am. Chem. Soc.* **1978**, *100*, 5659. (d) Post, D.; Baerends, E. J. *Chem. Phys. Lett.* **1982**, *86*, 176. (e) Cox, P. A.; Benard, M.; Veillard, A. *Chem. Phys. Lett.* **1982**, *87* 159. (f) Hay, P. J. *J. Am. Chem. Soc.* **1982**, *104*, 7007. (g) Messmer, R. P.; Caves, T. C.; Kao, C. M. *Chem. Phys. Lett.* **1982**, *90*, 296. (h) Böhm, M. C. *Int. J. Quantum Chem.* **1983**, *24*, 185. (i) Trogler, W. C. *J. Chem. Educ.* **1980**, *57*, 424.

(32) Cotton, F. A.; Davison, A.; Day, V. W.; Fredrich, M. F.; Orvig, C.; Swanson, R. *Inorg. Chem.* **1982**, *21*, 1211.

(33) Cotton, F. A. *Chem. Soc. Rev.* **1983**, *12*, 35.

(34) Yoo, C. S.; Zink, J. I. *Inorg. Chem.* **1983**, *22*, 2474.

(35) Figgis, B. N. "Introduction to Ligand Fields"; Wiley: New York, 1966; p 60.

pair combination with the metal–metal π bond is caused more by degeneracy than by overlap and bonding. One reason for this discrepancy between the mixing indicated by the calculations and by the experiment is probably the calculations' use of PH_3 to model PMe_3. Comparative SCM–Xα–DV calculations on PMe_3 and PH_3 show that the first ionization potential of PMe_3 should occur at 2 eV lower ionization energy than that of PH_3.[36] This shift is observed experimentally in the photoelectron spectra of PMe_3 and PH_3[37] and is sufficient to significantly reduce the metal–phosphorus mixing in the 8e and 9e orbitals.

The fourth ionization component in this region is a shoulder on the high binding energy side of the predominantly phosphorus 8e ionization. Within the context of our present information on the photoelectron spectra of metal–metal bonded complexes, this ionization can only be assigned to removal of an electron from the predominantly metal–metal σ valence orbital. The approximately 1 eV separation of this ionization from the π ionization is much the same as that observed in electron deficient triply bonded ($\sigma^2\pi^4$) metal complexes.[8,9] It is especially interesting to correlate this ionization with features in the spectra of the quadruply bonded tungsten and molybdenum analogues. One suggestion is that it has shifted from the region of numerous overlapping bands beginning at 10 eV and greater binding energy in the spectra of the tungsten and molybdenum complexes. The initial band at 10 eV is primarily associated with chlorine p_π orbitals. This band is at the same position (±0.1 eV) in the spectra of the Mo, W, and Re complexes. The spectra do show changes in the 10.5–11-eV region that indicate some metal character associated with these ionizations. However, assignment of the metal–metal σ ionization to this region would require a shift of over 1 eV to *lower* binding energy from the tungsten to the rhenium complex, which is opposite to the observations for the other predominantly metal ionizations. The metal character associated with the ionizations in the 10.5–11 eV region is more likely due to the deeper-lying M–Cl and M–P σ interactions.

The remaining explanation is that this metal–metal σ ionization correlates with one of the ionization bands in the low ionization energy valence region of the tungsten complex. Within the present set of observations the most likely band of the tungsten complex to be assigned to the σ ionization is the relatively sharp shoulder at 7.45 eV in the π ionization region. It was pointed out previously that this shoulder could result from complex spin–orbit interactions in the π ionization region of a quadruply bonded complex.[7] By symmetry, the $E_{1/2}$ component will couple with σ symmetry states and the $E_{3/2}$ component will couple with δ^* symmetry states.[7,11] In the tungsten complex these effects can be further complicated by interaction of configurations involving the low-lying virtual δ^* orbital.[11] However, in this rhenium case the δ^* orbital is occupied and the spectrum of the rhenium complex shows a normal spin–orbit splitting of the π ionization. Therefore the spin–orbit splitting of the π ionization in the tungsten complex, which should be smaller than the indicated splitting in the rhenium complex because of the smaller spin–orbit coupling parameter, is probably unresolved in the first broad band at 7.05 eV. This leaves the band at 7.45 eV in the spectrum of the tungsten complex for assignment to the σ ionization.

Assignment of the valence σ ionization energy close to the π ionization energy is consistent with recent photoelectron studies of metal–metal complexes with electron-poor triple bonds ($\sigma^2\pi^4$) and quadruple bonds ($\sigma^2\pi^4\delta^2$).[5,9] This assignment has important implications for understanding the interactions of two directly bonded metal atoms. The close proximity of these ionizations is much different than the expectations based on the SCF–Xα calculations of $Re_2Cl_4(PH_3)_4$, which place the σ orbital energy at least 6 eV deeper than the π orbital energy.[10] A similar problem exists for metal–metal quadruply bonded systems. SCF–Xα–SW calculations consistently indicate stable valence σ orbital energies with relatively large σ–π ionization energy separations.[7,38]

Other calculations, all of which use some form of the LCAO approach, generally place the σ and π ionizations within 1 eV.[39,40] It has recently been pointed out, on the basis of related experimental and theoretical work,[9,39] that one factor likely to be important in these considerations is the interaction of the valence σ density on one metal atom (rhenium $5d_{z^2}$) with the outer core density on the neighboring metal atom (rhenium 5s, $5p_z$, and perhaps 4f). It might be noted that core–core repulsions involving the outer core p shells have been discussed as a factor determining metal–metal bond lengths in these multiply bonded systems.[41] The interaction of valence d_{z^2} density on one metal with the outer core p_z density on the next metal is likely to be more substantial than the core–core interactions. Additional theoretical evidence of the significance of outer core p orbital interactions in these systems is provided by a recent ab initio study of short metal–metal bonds employing pseudopotentials to represent the core electrons.[42] This study found that the outer core p shell must be explicitly included in the self-consistent cycle. The appreciable overlap between the valence d_{z^2} obitals and the outer core p_z orbitals on close neighboring metal atoms tends to shift the valence σ ionization to lower binding energy and reduce the bond distance change that occurs with removal of a σ valence electron. This interaction will be slightly more important for tungsten atoms than for the smaller rhenium atoms. The effect, in combination with the inherently more stable rhenium orbitals, contributes to shifting the valence σ ionization of the rhenium complex to about 1.4 eV greater ionization energy than the corresponding ionization of the tungsten complex. The SCF–Xα–SW calculations are apparently unable to fully account for these very directional σ valence-core interactions, possibly because of the use of overlapping atomic spheres within which a spherically symmetric potential is assumed. Additional studies are underway to further characterize the nature of these metal–metal interactions.

Summary

An examination of the redox behavior and reactivity patterns of the triply bonded d^5–d^5 complexes $Re_2X_4(PMe_3)_4$ (X = Cl or Br) have led to the isolation of the paramagnetic salts $[Re_2X_4(PMe_3)_4]PF_6$ and the mixed ligand complexes $Re_2Cl_4(PMe_3)_2(LL)$ (LL = $Ph_2PCH_2PPh_2$ (dppm) or $Ph_2PNHPPh_2$ (dppa)). NMR spectral studies on the latter neutral species have convincingly established their structure (see II). The volatility of the complex $Re_2Cl_4(PMe_3)_4$ has, for the first time, permitted the measurement of the gas-phase photoelectron spectrum of a complex of this type. This shows a clear $\sigma^2\pi^4\delta^2\delta^{*2}$ configuration for the electron-rich metal–metal triple bond in $Re_2Cl_4(PMe_3)_4$. The separations of the δ^*, δ, and π ionizations are in excellent agreement with the results of SCF–Xα calculations. The relative widths of the δ^* and δ ionizations are consistent with their antibonding and bonding characters, although the major contributions to these bandwidths come from sources other than the metal–metal bond order. The π ionization shows evidence of spin–orbit splitting into equal components that is typical of an e orbital with high metal character. The ionization shoulder at 8.8 eV, which we discuss in terms of removal of an electron from the metal–metal valence σ orbital, is especially intriguing. The placement of this ionization is consistent with that of electron-poor metal–metal triple bonds and correlates with the sharp ionization feature in the π ionization region of the tungsten complex. Observation of this ionization

(36) Xiao, S.-X.; Trogler, W. C.; Ellis, D. E.; Berkovitch-Yellin, Z. *J. Am. Chem. Soc.* **1983**, *105*, 7033.

(37) Maier, J. P.; Turner, D. W. *J. Chem. Soc., Faraday Trans. 2* **1972**, *68*, 711.

(38) (a) Cotton, F. A.; Kalbacher, B. J. *Inorg. Chem.* **1977**, *16*, 2386. (b) Norman, J. G., Jr.; Kolari, H. J.; Gray, H. B.; Trogler, W. C. *Ibid.* **1977**, *16*, 987. (c) Norman, J. G., Jr.; Kolari, H. J. *J. Am. Chem. Soc.* **1975**, *97*, 33. (d) Bursten, B. E.; Cotton, F. A.; Fanwick, P. E.; Stanley, G. G. *Ibid.* **1983**, *105*, 3082.

(39) (a) Ziegler, T. *J. Am. Chem. Soc.* **1984**, *106*, 5901. (b) Ziegler, T. *Ibid.* **1985**, *107*, 4453.

(40) (a) Manning, M. C.; Holland, G. F.; Ellis, D. E.; Trogler, W. C. *J. Phys. Chem.* **1983**, *87*, 3083. (b) Guest, M. F.; Garner, C. D.; Hillier, I. H.; Walton, I. B. *J. Chem. Soc. Faraday Trans. 2* **1978**, *74*, 2092. (c) Hillier, I. H.; Garner, C. D.; Mitcheson, G. R.; Guest, M. F. *J. Chem. Soc., Chem. Commun.* **1978**, 204.

(41) (a) Reference 2, pp 347–351. (b) McLean, A. D.; Liu, B. *Chem. Phys. Lett.* **1983**, *101*, 144.

(42) Bernholc, J.; Holzworth, N. A. W. *Phys. Rev. Lett.* **1983**, *50*, 1451.

provides experimental support for LCAO-MO calculations, which place this valence σ ionization in close proximity to the π ionization. The complete interpretation of this state has important implications for the understanding of metal-metal interactions. An important factor contributing to the energy of the valence σ ionization appears to be direct interaction between the valence σ orbital density ($5d_{z^2}$) on one metal and the "core" (5s, $5p_z$) density on the neighboring metal atom.

Acknowledgments. We thank the Nationl Science Foundation (Grant No. CHE82-06117 to R.A.W. and CHE82-06169 to A.P.S.) and the Department of Energy (Contract No. DE-AC02-80ER10746 to D.L.L.) for support of this work. We appreciate the assistance of Stephen M. Tetrick in the measurement and interpretation of the NMR spectra, Arlene Rothwell for obtaining the EI and CI mass spectra, and Ann Copenhaver for analyzing the PE data.

Electronic and Vibrational Spectroscopy of the Triply Metal-Metal Bonded $Mo_2(HPO_4)_4^{2-}$ Ion. Inferences as to the Energetics of δ-Bonding from Spectroscopic Correlations to $Mo_2(SO_4)_4^{4-/3-}$

Michael D. Hopkins, Vincent M. Miskowski,* and Harry B. Gray*

Contribution No. 7273 from the Arthur Amos Noyes Laboratory, California Institute of Technology, Pasadena, California 91125. *Received August 26, 1985*

Abstract: Room- and low-temperature polarized single-crystal absorption spectra are reported for the triply metal-metal bonded $(pyH)_3[Mo_2(HPO_4)_4]Cl$ complex between 300 and 800 nm, and spectra to both higher and lower energy than this wavelength range are reported for a low-temperature pellet of $Cs_2[Mo_2(HPO_4)_4]\cdot 2H_2O$. Absorptions at 420, 542, and 670 nm in the single-crystal spectrum are assigned on the basis of their polarization and temperature behavior, as well as by comparison to previously unassigned bands in the spectra of $K_3[Mo_2(SO_4)_4]\cdot 3.5H_2O$ and $K_4[Mo_2(SO_4)_4]\cdot 2H_2O$, to $^1(\pi \rightarrow \delta^*)$, $^1(\pi \rightarrow \delta)$, and $^3(\pi \rightarrow \delta)$, respectively. A band at 340 nm, which is not observed in the pellet spectrum of the Cs^+ salt or in solution, is assigned to $\sigma(Mo-Cl) \rightarrow \delta(Mo_2)$ LMCT, while an intense absorption at 250 nm in the pellet spectrum is tentatively attributed to the $^1(\pi \rightarrow \pi^*)(Mo_2)$ transition. A Faraday magnetic measurement supports the proposed ($\sigma^2\pi^4$) triple-bond ground state of $Mo_2(HPO_4)_4^{2-}$, which displays the Raman-active $\nu(Mo_2)$ vibration at ~ 360 cm^{-1} for both salts. The differences in observed metal-metal stretching frequencies and the observed and calculated one-electron splitting of the δ and δ^* levels of the Mo_2(III,III) phosphate and Mo_2(II,III) and Mo_2(II,II) sulfate complexes are entirely consistent with the change in formal metal-metal bond order from 3 to 4 across this series.

Spectroscopic studies of the $^1(\delta \rightarrow \delta^*)$ transition of quadruply bonded metal dimers have been of central importance in elucidating the electronic structural details of the δ-bond present in this class of compounds.[1,2] One of the principal themes that has emerged from consideration of the overall spectral behavior of these systems is that the relatively high energy and low intensity of this transition are a direct consequence of the weak overlap of the d_{xy} orbitals that comprise the δ-interaction.[1] The actual contribution of the energetic splitting of the one-electron δ and δ^* levels to the energy of the $^1(\delta\delta^*)$ state, however, has been difficult to assess experimentally,[3-5] and hence quantitative spectroscopic measurements of the extent to which the δ-interaction is perturbed by such variables as metal-metal distance, metal-ligand interactions, and formal charge of the M_2 unit have, for the most part, remained elusive.

Binuclear complexes that span a wide range of d-electron counts and formal metal-metal bond orders have been prepared and structurally characterized, particularly over the last 25 years.[2] Several years ago, compounds containing the $Mo_2(SO_4)_4^{4-/3-}$ ions, which constitute examples of bond orders of 4($\sigma^2\pi^4\delta^2$) and 3.5-($\sigma^2\pi^4\delta^1$), respectively, were reported[6] and subsequently thoroughly characterized with respect to their spectroscopic properties.[7-11] This series has recently been extended to include an example with a formal bond order of 3 with the discovery of the structurally related $Mo_2(HPO_4)_4^{2-}$ ion,[12,13] which is proposed to possess a ($\sigma^2\pi^4\delta^0$) electronic configuration. Comparisons of the molecular structures of these three compounds show that the major perturbation to the Mo_2O_8 core across this series is a small, monotonic increase in the metal-metal distance with decreasing bond order ($\sim$0.06 Å/δ electron),[12] as anticipated from qualitative electronic structural considerations. We report herein the results of our electronic and vibrational spectroscopic investigation of the $Mo_2(HPO_4)_4^{2-}$ ion, as well as the correlation of the relative energies of the π, δ, and δ^* levels with metal oxidation state and metal-metal distance for this class of complexes.

Experimental Section

General Procedures. All chemicals were of reagent grade or comparable quality and were used as received. Elemental analyses were performed by Mr. Larry Henling at the Caltech Analytical Laboratory. Magnetic susceptibilities were obtained at room temperature with a Faraday balance that was calibrated with $HgCo(SCN)_4$. Raman spectra

(1) Trogler, W. C.; Gray, H. B. *Acc. Chem. Res.* **1978**, *11*, 232-239.
(2) Cotton, F. A.; Walton, R. A. "Multiple Bonds Between Metal Atoms"; Wiley: New York, 1982.
(3) Hopkins, M. D.; Zietlow, T. C.; Miskowski, V. M.; Gray, H. B. *J. Am. Chem. Soc.* **1985**, *107*, 510-512.
(4) Campbell, F. L., III; Cotton, F. A.; Powell, G. L. *Inorg. Chem.* **1985**, *24*, 177-181.
(5) Manning, M. C.; Trogler, W. C. *J. Am. Chem. Soc.* **1983**, *105*, 5311-5320.
(6) Bowen, A. R.; Taube, H. *J. Am. Chem. Soc.* **1971**, *93*, 3287-3289. Bowen, A. R.; Taube, H. *Inorg. Chem.* **1974**, *13*, 2245-2249. Cotton, F. A.; Frenz, B. A.; Pedersen, E.; Webb, T. R. *Inorg. Chem.* **1975**, *14*, 391-398.
(7) Angell, C. L.; Cotton, F. A.; Frenz, B. A.; Webb, T. R. *J. Chem. Soc., Chem. Commun.* **1973**, 399-400.
(8) Loewenschuss, A.; Shamir, J.; Ardon, M. *Inorg. Chem.* **1976**, *15*, 238-241.
(9) Cotton, F. A.; Martin, D. S.; Fanwick, P. E.; Peters, T. J.; Webb, T. R. *J. Am. Chem. Soc.* **1976**, *98*, 4681-4682.
(10) Erwin, D. K.; Geoffroy, G. L.; Gray, H. B.; Hammond, G. S.; Solomon, E. I.; Trogler, W. C.; Zagars, A. A. *J. Am. Chem. Soc.* **1977**, *99*, 3620-3621.
(11) Fanwick, P. E.; Martin, D. S.; Webb, T. R.; Robbins, G. A.; Newman, R. A. *Inorg. Chem.* **1978**, *17*, 2723-2727.
(12) Bino, A.; Cotton, F. A. *Angew. Chem., Int. Ed. Engl.* **1979**, *18*, 462-463. Bino, A.; Cotton, F. A. *Inorg. Chem.* **1979**, *18*, 3562-3565.
(13) Bino, A. *Inorg. Chem.* **1981**, *20*, 623-626.

0002-7863/86/1508-0959$01.50/0